

RESEARCH ARTICLE

# Model-based quantification of metabolic interactions from dynamic microbial-community data

Mark Hanemaaijer<sup>1,2</sup>, Brett G. Olivier<sup>1</sup>, Wilfred F. M. Röling<sup>2</sup>, Frank J. Bruggeman<sup>1</sup>, Bas Teusink<sup>1\*</sup>

**1** Systems Bioinformatics, Amsterdam Institute for Molecules, Medicines and Systems, VU Amsterdam, The Netherlands, **2** Molecular Cell Physiology, Amsterdam Institute for Molecules, Medicines and Systems, VU Amsterdam, The Netherlands

\* [b.teusink@vu.nl](mailto:b.teusink@vu.nl)



**OPEN ACCESS**

**Citation:** Hanemaaijer M, Olivier BG, Röling WFM, Bruggeman FJ, Teusink B (2017) Model-based quantification of metabolic interactions from dynamic microbial-community data. PLoS ONE 12 (3): e0173183. doi:10.1371/journal.pone.0173183

**Editor:** Stephen S. Fong, Virginia Commonwealth University, UNITED STATES

**Received:** September 6, 2016

**Accepted:** February 16, 2017

**Published:** March 9, 2017

**Copyright:** © 2017 Hanemaaijer et al. This is an open access article distributed under the terms of the [Creative Commons Attribution License](https://creativecommons.org/licenses/by/4.0/), which permits unrestricted use, distribution, and reproduction in any medium, provided the original author and source are credited.

**Data Availability Statement:** All relevant data are within the paper and its Supporting Information files and on [https://sourceforge.net/projects/cbmpy/files/publications/data/2017\\_Hanemaaijer/](https://sourceforge.net/projects/cbmpy/files/publications/data/2017_Hanemaaijer/).

**Funding:** This work is financially supported by ZonMW and the Netherlands Genomics Initiative via a Zenith Horizon grant 40-41009-98-10038. BGO is supported by a BE-Basic Foundation grant F08.005.001.

**Competing interests:** The authors have declared that no competing interests exist.

## Abstract

An important challenge in microbial ecology is to infer metabolic-exchange fluxes between growing microbial species from community-level data, concerning species abundances and metabolite concentrations. Here we apply a model-based approach to integrate such experimental data and thereby infer metabolic-exchange fluxes. We designed a synthetic anaerobic co-culture of *Clostridium acetobutylicum* and *Wolinella succinogenes* that interact via interspecies hydrogen transfer and applied different environmental conditions for which we expected the metabolic-exchange rates to change. We used stoichiometric models of the metabolism of the two microorganisms that represents our current physiological understanding and found that this understanding - the model - is sufficient to infer the identity and magnitude of the metabolic-exchange fluxes and it suggested unexpected interactions. Where the model could not fit all experimental data, it indicates specific requirement for further physiological studies. We show that the nitrogen source influences the rate of interspecies hydrogen transfer in the co-culture. Additionally, the model can predict the intracellular fluxes and optimal metabolic exchange rates, which can point to engineering strategies. This study therefore offers a realistic illustration of the strengths and weaknesses of model-based integration of heterogenous data that makes inference of metabolic-exchange fluxes possible from community-level experimental data.

## Introduction

Microbial communities carry out important processes for the planet's ecosystem, animal health and industrial purposes. Engineering such communities is not straightforward; they are generally composed of many interacting microorganisms, and they are highly dynamic. Developing methods that relate the systemic properties of communities to the underlying metabolic processes and interactions of the community members is a major challenge in microbial ecology. Those interactions drive community behaviour, including its (in-)stability upon

environmental perturbations [1]. Metabolic interactions between community members are widespread and generally considered to be the dominating interactions [2–4].

Current approaches focus mostly on correlation and co-occurrence of species members for inference of community-interaction partners [5, 6]. These approaches importantly predict the community-interaction structure, even for large systems. It does not, however, inform us about interaction mechanisms and their importance for species survival and community properties. This can be achieved when we know the metabolic exchange fluxes between microorganisms; then we would capture both mechanism and importance of those fluxes, as those can be linked to intracellular metabolic activities and growth. With this additional information we could rationally design approaches that alter community behaviour upon external perturbations.

Unfortunately, quantifying metabolic exchange fluxes—metabolic interactions—directly from experimental data is rarely possible. Generally, only net fluxes are inferred from dynamic metabolite levels measured at the community level that result from contributions of many species. To determine the individual contributions of those species, we suggested that their metabolic capacities, expressed in terms of quantitative models, should be integrated with experimental data [7]. Here we illustrate that this indeed allows for the identification and quantification of metabolic interactions between microorganisms and that those interactions are dependent on environmental conditions.

Our approach relies on stoichiometric models of metabolism and the linkage of the metabolism of microbial species in the community. Stoichiometric modeling of the metabolism of single microorganisms have been developed in systems biology in the last two decades. Recently, such models are being considered for microbial communities [8–11], but the number of studies that combine such metabolic models with experimental data is still limited. The first study was performed by Stolyar *et al.* on a methanogenic co-culture [12] and several other co-culture studies followed [13, 14]. Also, purely computational studies investigated the potential interactions in a community [15], designed medium compositions that enforces metabolic interactions [16] or calculated biomass ratios and fluxes under balanced growth conditions of microbial communities [17]. The focus of those studies was mostly the prediction of the community phenotype. However, another application of those models is to use them to infer metabolic exchange fluxes between microorganisms from experimental data [7].

Here we demonstrate that we are able to quantify community interactions by combining experimental data, consisting of biomass abundances and metabolite concentrations, with stoichiometric metabolism models. For this purpose, we designed a synthetic co-culture that serves as a model for anaerobic interspecies hydrogen transfer, which is one of the driving forces in the anaerobic digestion process, and allows for tunable metabolic interactions by changing the environmental conditions. Quantification of the metabolic interactions contributes to identifying how this important process can be improved. Although synthetic communities are not as complex as natural ecosystems, they have shown to be useful for microbial ecologists to examine ecological theories, such as the influence of community evenness on the functionality of a community [18]. Additionally, synthetic communities are used to improve industrial applications, such as bioremediation [19] or bioethanol production [20]. The co-culture we designed consists of the anaerobic bacteria *Clostridium acetobutylicum* and *Wolinella succinogenes*. *C. acetobutylicum* produces  $H_2$  that subsequently is consumed by *W. succinogenes* to reduce nitrate ( $NO_3^-$ ) into nitrite ( $NO_2^-$ ) or ammonium ( $NH_4^+$ ).  $NO_2^-$  or  $NH_4^+$  can act as a nitrogen-source for *C. acetobutylicum*. We varied the nitrogen source to vary the metabolic interactions in the community, which we subsequently inferred, using a model and experimental data. This study illustrates how the integration of a model, representing our knowledge

about the metabolism of the two species, with experimental data leads to the quantification of metabolic exchange fluxes.

## Materials and methods

### Strains and cultivation conditions

Co-culture experiments of *Clostridium acetobutylicum* DSM-792 with *Wolinella succinogenes* DSM-1740 were grown in Widdel-based medium containing the following components (per liter): 1 g NaCl, 0.4 g MgCl $\cdot$ 6H $_2$ O, 0.1 g CaCl $\cdot$ 2H $_2$ O, 0.5 g KCl, 0.59 g glucose $\cdot$ H $_2$ O, 0.15 g cysteine, supplemented with 1 ml of 100x RPMI-1640 vitamin solution (Sigma-Aldrich) and 1 ml of trace elements solution, containing (per liter): 0.5 g EDTA, 3 g MgSO $_4$  $\cdot$ 7H $_2$ O, 0.5 g MnSO $_4$  $\cdot$ H $_2$ O, 1 g NaCl, 0.1 g FeSO $_4$  $\cdot$ 7H $_2$ O, 0.1 g Co(NO $_3$ ) $_2$  $\cdot$ 6H $_2$ O, 0.1 g CaCl $_2$ , 0.1 g ZnSO $_4$  $\cdot$ 7H $_2$ O, 10 mg CuSO $_4$  $\cdot$ 5H $_2$ O, 10 mg AlK(SO $_4$ ) $_2$ , 10 mg H $_3$ BO $_3$ , 10 mg Na $_2$ MoO $_4$  $\cdot$ 2H $_2$ O, 1 mg Na $_2$ SeO $_3$ , 10 mg Na $_2$ WO $_4$  $\cdot$ 2H $_2$ O, 20 mg NiCl $_2$  $\cdot$ 6H $_2$ O. A 20 mM Na-phosphate buffer pH 7.0 was used to maintain a constant pH during the growth experiment. The final pH of the medium was 7.0. The medium was kept anaerobic by flushing with a gas mixture of 10% CO $_2$  and 90% N $_2$ . Resazurine (0.01 mg/l) was used as an indicator for anaerobic conditions. The growth experiment was performed at 37°C in 100 ml septum vials with rubber stoppers containing 50 ml of growth medium. 'NH $_4^+$ ' condition contained 0.25 g/L NH $_4$ Cl, 'NO $_3^-$ ' condition contained 0.85 g/l NaNO $_3^-$ , 'NH $_4^+$  + NO $_3^-$ ' condition contained 0.25 g/l NH $_4$ Cl and 0.85 g/l NaNO $_3^-$  and 'N $_2$ ' condition contained no N-source, except N $_2$  in the headspace. Cells were taken from actively growing stock, cultivated in monoculture first in abovementioned medium, but with yeast extract supplemented. The monocultures were added 1:1 (OD/OD) in the media, pre-grown for 70 generations via serial transfer of the co-culture in NH $_4^+$  + NO $_3^-$  containing medium to create a stable co-culture. We are aware that mutations could arise during this period which potentially influence the community phenotype, but that is beyond the scope of this study. The co-culture was 1:100 propagated to fresh medium once it was fully grown. The experiment started when the co-culture reached exponential growth and was 1:100 propagated to fresh medium containing different nitrogen sources in triplicate.

### Metabolite analysis

Supernatant from the batch cultivation was taken from the septum vials by taking 1 ml of growth medium and filtered through a 0.2  $\mu$ m polyethersulfone (PES) filter and stored at -20°C until further processing. Samples were analyzed for fermentation products (i.e. formate, succinate, acetate, propionate, lactate, and butyrate) by high performance liquid chromatography (HPLC) with a Phenomenex Rezex ROA 300x7.8mm column at 55°C and occupied with RID 10A and SPD 20A detectors having a flow rate of 0.5ml/min and eluent of 5mM H $_2$ SO $_4$ . NO $_3^-$  was measured according Yang et al. [21] and NO $_2^-$  was measured spectrophotometrically at 520nm by diazotization of sulphanilamide by nitrite. CO $_2$  and H $_2$  were measured by taking 100  $\mu$ l gas sample from the head space with a syringe (Terumo 1 mL syringe) and the gas was immediately analyzed on a Shimadzu GC2010 system equipped with a Carboxen 1010 column (30m $\cdot$ 0.58mm, 105°C) and a barrier discharge ionization detector (BID). Helium was used as a carrier gas at 28.2 mL/min at a pressure of 37.2 kPa.

### Quantification of cells

DNA was extracted with the PowerSoil DNA isolation kit (MO BIO Laboratories, Solana Beach, CA, USA), according the manufacturer protocol, from 2 ml of culture. Species abundance was measured by quantitative PCR using primers for *C. acetobutylicum* [22] and *W.*

*succinogenes* (forward primer (5'→3'): CCACACGACACTACCCTCAC and reverse primer (5'→3'): CGGTGCTTACGATTCCCAGT) on a 7300 Real Time PCR System (AB Applied Biosystems, CA, USA). Both primer sets are selective for the target species and the quantification of genes is corrected with the number of genes on the genome. The following PCR program was used for *C. acetobutylicum* quantification: a start-up step of 50°C for 2 minutes, followed by an initial denaturation step at 94°C for 10 minutes, 40 cycles of 94°C for 30 seconds, 54°C for 30 seconds and 72°C for 40 seconds, plus a final elongation step at 72°C for 5 minutes. For quantification of *W. succinogenes* we used: a start-up step of 50°C for 2 minutes, followed by an initial denaturation step at 94°C for 10 minutes, 45 cycles of 94°C for 10 seconds, and 60°C for 30 seconds.

## Models and software

All simulations were done using CBMPy 0.7.0 (<http://cbmpy.sourceforge.net/>), a Python-based software package. The genome-scale metabolic model of *C. acetobutylicum* [13], a coarse-grained metabolic model and a genome-scale metabolic model of *W. succinogenes* (see supplements), using the SBML level 3 standards [23], were used to perform the simulations (All models and scripts are available on [https://sourceforge.net/projects/cbmpy/files/publications/data/2017\\_Hanemaaijer/](https://sourceforge.net/projects/cbmpy/files/publications/data/2017_Hanemaaijer/)). The method to reconstruct the genome-scale metabolic model of *W. succinogenes* is described in the supplemental material. Dynamic flux balance analysis simulations were based on the method by Zhuang *et al.* [24], but implemented in Python using the LSODA integrator provided by the SciPy scientific library [25]. The CPLEX-solver (academic license) from IBM<sup>®</sup> was used for optimization of the metabolic networks. The method for model reconstruction and co-culture growth simulations are described in the supplements. The Flux Variability Analysis was performed according Mahadevan *et al.* [26].

## Results

### Design of co-culture and media composition that gives rise to different metabolic interactions

We designed a synthetic co-culture of *C. acetobutylicum* and *W. succinogenes*, serving as a model system for anaerobic interspecies hydrogen transfer. These species are chosen, because they allow for tunable metabolic interactions by changes made to the medium composition, in particular the nitrogen source (Fig 1).

We choose *C. acetobutylicum* because it produces H<sub>2</sub> from glucose, which can be consumed by *W. succinogenes* to generate energy for the reduction of NO<sub>3</sub><sup>-</sup> to NO<sub>2</sub><sup>-</sup> or, further, to NH<sub>4</sub><sup>+</sup> when the NO<sub>3</sub><sup>-</sup> concentration is low. We choose a high NO<sub>3</sub><sup>-</sup> concentration in our experimental set-up to prevent this. As an alternative to H<sub>2</sub> *W. succinogenes* can use formate. Since *C. acetobutylicum* cannot use NO<sub>3</sub><sup>-</sup> as a nitrogen-source it has to fix N<sub>2</sub> gas when NO<sub>3</sub><sup>-</sup> is the sole nitrogen source in pure culture [27]. However, in co-culture *C. acetobutylicum* can use NO<sub>2</sub><sup>-</sup> produced by *W. succinogenes*. Alternatively, when NH<sub>4</sub><sup>+</sup> is present, both organisms can use it as nitrogen source, but *W. succinogenes* would still not grow because it lacks an energy source. Varying the nitrogen source also has additional effects. When NH<sub>4</sub><sup>+</sup> and NO<sub>3</sub><sup>-</sup> is present, *C. acetobutylicum* is independent of *W. succinogenes* and supplies H<sub>2</sub> to *W. succinogenes*. *C. acetobutylicum* becomes dependent on *W. succinogenes* when only NO<sub>3</sub><sup>-</sup> is present. Then *W. succinogenes* cross feeds NO<sub>2</sub><sup>-</sup> to *C. acetobutylicum*, which, in turn, supplies H<sub>2</sub> that facilitates NO<sub>3</sub><sup>-</sup> to NO<sub>2</sub><sup>-</sup> reduction by *W. succinogenes*. Thus we can design co-cultures with uni- and bidirectional metabolic interactions. We studied four different conditions; the associated, expected metabolic interactions are shown in Fig 1.

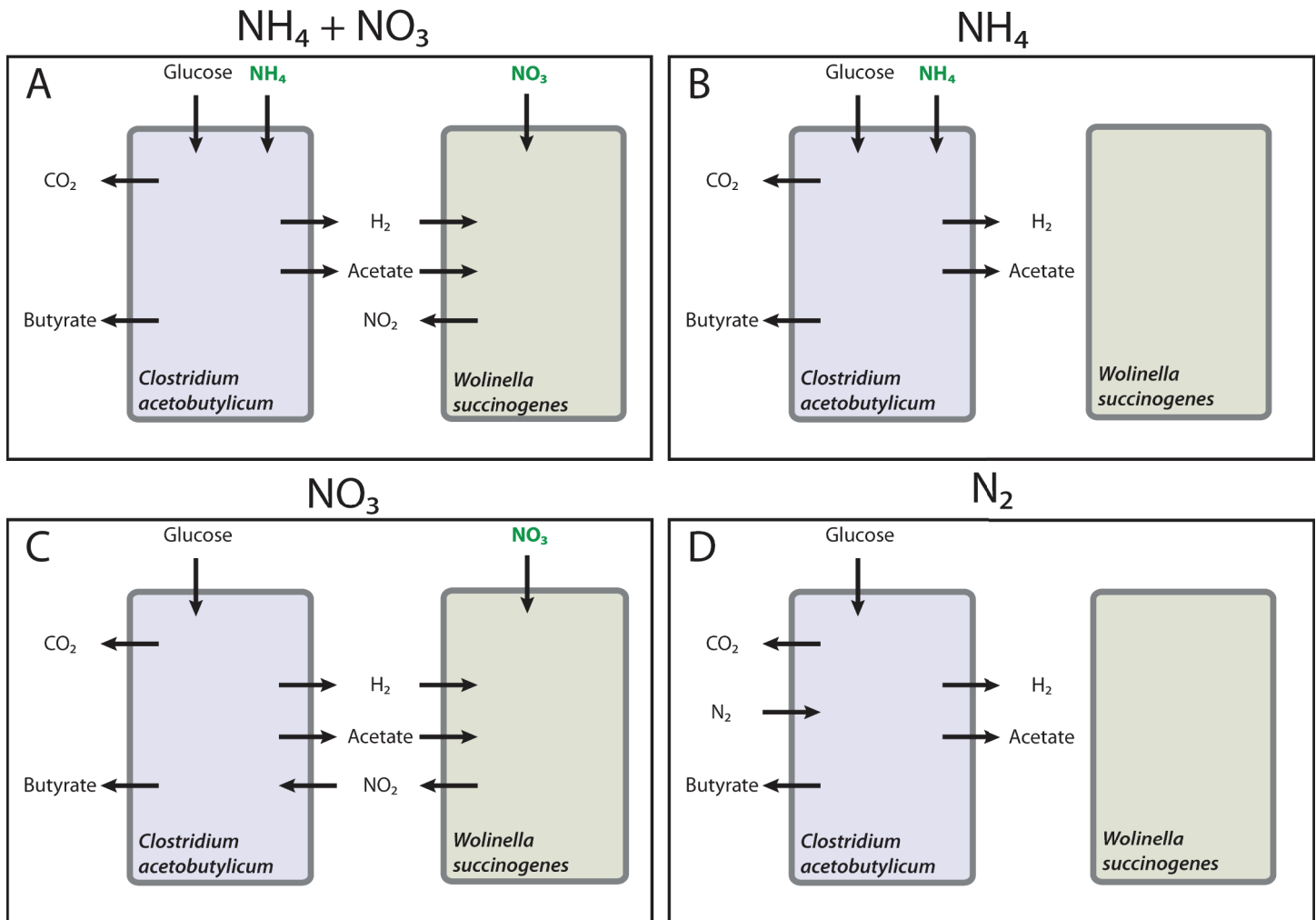


**Fig 1. Source of nitrogen is expected to influence the metabolic interactions between *C. acetobutylicum* and *W. succinogenes*.** **A** shows the expected interactions between *C. acetobutylicum* and *W. succinogenes* in the presence of  $\text{NH}_4^+$  and  $\text{NO}_3^-$ . **B** shows the interactions in the presence of only  $\text{NH}_4^+$ , **C** in the presence of only  $\text{NO}_3^-$  and **D** shows the expected interactions in the presence of only  $\text{N}_2$ . Although we expect certain interactions in the co-culture during the various environmental conditions, we do not know at what rate the metabolites are exchanged.

doi:10.1371/journal.pone.0173183.g001

### Experimental data of four growth conditions

The co-culture was grown in four different environmental conditions, in which we varied the nitrogen-source to study its influence on the state of the community, outlined in Fig 1. The media either contained  $\text{NH}_4^+$  and  $\text{NO}_3^-$ , only  $\text{NH}_4^+$ , only  $\text{NO}_3^-$  or neither.  $\text{N}_2$  was the only nitrogen-source in the absence of  $\text{NH}_4^+$  and  $\text{NO}_3^-$ , with the expectation that only *C. acetobutylicum* can grow. Across conditions, the biomass abundances and metabolite concentrations were measured in time to study the impact of the nitrogen-source on the co-culture dynamics.

The different conditions influenced the growth and metabolic profiles of the co-culture (Fig 2). The co-culture grew slower in the  $\text{N}_2$  condition and led to a 2-fold lower optical density than the  $\text{NO}_3^-$  condition (Fig 2A). In the  $\text{N}_2$  condition, *C. acetobutylicum* fixes  $\text{N}_2$  gas to acquire nitrogen, which is an energetically unfavourable process [28, 29]. The  $\text{N}_2$  condition

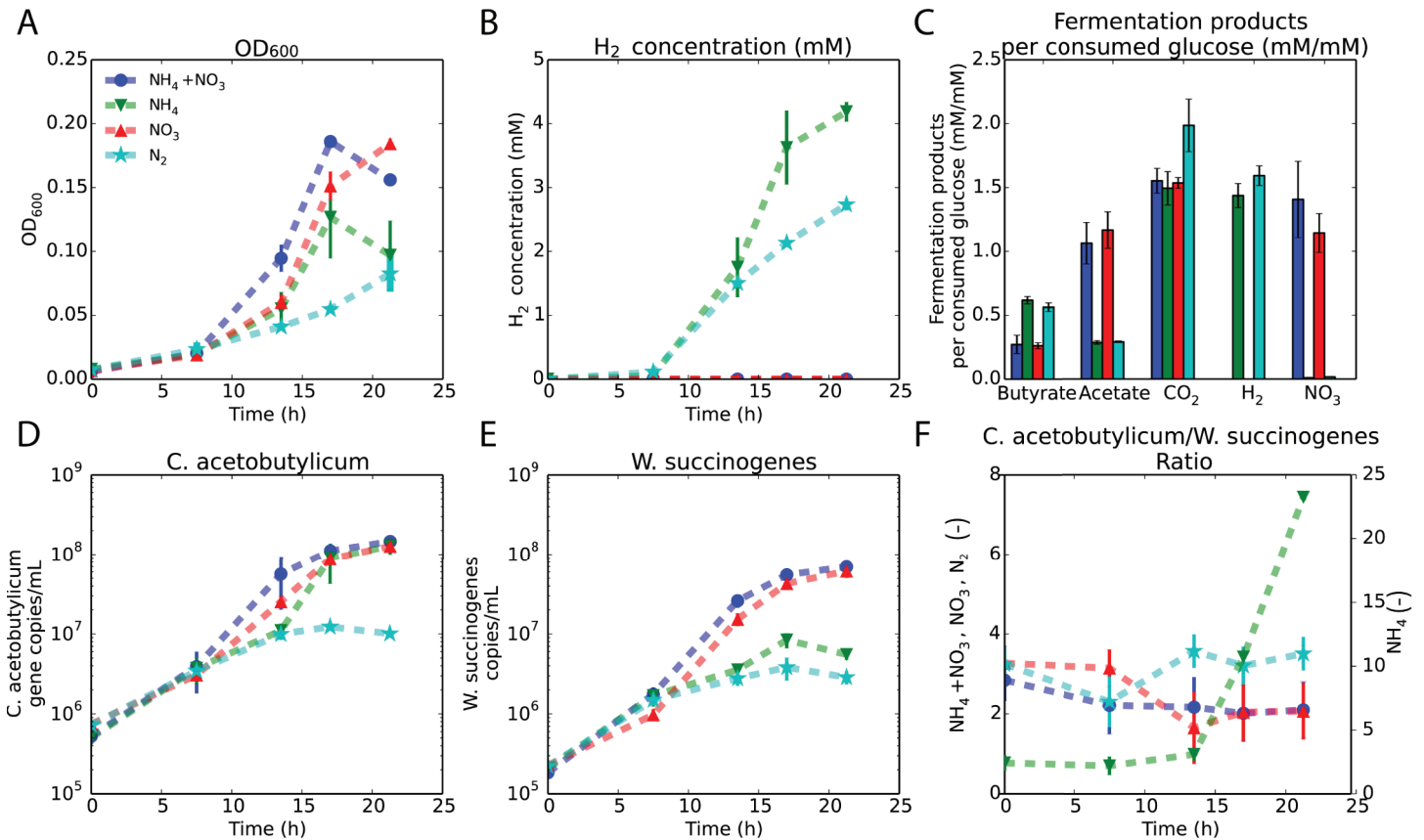


**Fig 2. Nitrogen-source alters the phenotypic behaviour of the co-culture in batch experiments.** **A** shows optical density measurements at 600 nm. **B** is the measured  $H_2$  concentrations. **C** are fermentation products per consumed glucose at the end of the cultivation period and is the sum of the production and consumption of the species in the co-culture. The  $NO_3^-$  is the amount of  $NO_3^-$  reduced. **D** and **E** are the quantified gene copies concentration per mL of *C. acetobutylicum* and *W. succinogenes*. **F** shows the ratios of *C. acetobutylicum* and *W. succinogenes* based on gene-copy number. This is to show that both strains show balanced growth during batch cultivation. The copy numbers are corrected for the amount of genes on the genome.

doi:10.1371/journal.pone.0173183.g002

was also the only condition where glucose was not completely consumed at the end of the experiment. A drop in the optical density was observed in two conditions at the end of the experiment, because of induction of sporulation by *C. acetobutylicum*. We only detected  $H_2$  when  $NO_3^-$  was absent (Fig 2B), suggesting that *W. succinogenes* consumed all the  $H_2$  produced by *C. acetobutylicum* in the presence of  $NO_3^-$  (since no formate was detected). The final amounts of butyrate, acetate,  $CO_2$  (produced by *C. acetobutylicum*) and reduced  $NO_3^-$  (by *W. succinogenes*) varied between the different conditions (Fig 2C). In the absence of  $NO_3^-$ , more butyrate was formed out of glucose, at the expense of acetate. This indicates a bidirectional interaction: in the presence of  $NO_3^-$ , when *W. succinogenes* grows, the  $H_2$  concentration is kept low by *W. succinogenes*, such that *C. acetobutylicum* has a different fermentation profile due to alleviation of  $H_2$ -inhibition, which is consistent with literature [30]. This is therefore proof of a bidirectional interaction, because *C. acetobutylicum* behaves as in pure culture in the absence of  $NO_3^-$ , with high  $H_2$  and butyrate concentrations. Note that  $H_2$  accumulates in the absence of  $NO_3^-$ , because the growth rate of *W. succinogenes* decreases (Fig 2E). *C. acetobutylicum* produced 30% more  $CO_2$  from glucose in the ' $N_2$ ' condition relative to the other conditions.

Fig 2F indicates time periods during which a constant biomass ratio of the two species were observed. Only in the presence of  $\text{NH}_4^+$ , *W. succinogenes* was outgrown by *C. acetobutylicum* after 13.5 hours, because no  $\text{NO}_3^-$  is available for *W. succinogenes* to convert  $\text{H}_2$ . In the other cases we found constant biomass ratios, always after 13.5 hours of cultivation, indicating that the two microorganisms grew at the same specific rate. Equal specific growth rates indicate that the growth of the two organisms was coupled. Such growth coupling can either result from bidirectional exchange of growth-supporting metabolites, or a unidirectional exchange from the slower-growing to the faster-growing microorganism. A bidirectional exchange was expected in the presence of only  $\text{NO}_3^-$ , whereas in the presence of  $\text{NH}_4^+$  and  $\text{NO}_3^-$  a unidirectional exchange was expected. Coupling occurs because the microorganism that is capable of a higher growth rate becomes limited by the other organism, which cannot supply its resources fast enough.

Which metabolites are exchanged and at what rate across those conditions cannot be deduced directly from the experimental data. For instance, we cannot conclude whether *C. acetobutylicum* only consumed  $\text{NH}_4^+$ , or that  $\text{NO}_2^-$  was also consumed in the presence of  $\text{NH}_4^+$  and  $\text{NO}_3^-$ . Also the  $\text{H}_2$  production rate of *C. acetobutylicum* remains unknown, as we could not detect  $\text{H}_2$  in two of the four conditions. Even though we can conclude that the species do exchange metabolites with each other, as they grew equally fast, we are not sure which metabolites are being exchanged let alone at what rate. To address those questions we analysed our experimental data with metabolic models of the two species.

## Stoichiometric models of co-culture metabolism and growth

We used stoichiometric metabolic models of *C. acetobutylicum* and *W. succinogenes* to fit the experimental data for the inference of metabolic interactions between the species during different environmental conditions. The metabolic models only describe the stoichiometry of metabolic reactions, based on genomic and biochemical information, and do therefore not contain any kinetic parameters of all the individual enzymes. In addition, we took the growth rates and the biomass abundances of the microorganisms into account to capture the metabolism and the dynamics of the co-culture, using an existing method called dynamic flux balance analysis (dFBA) [31], which extends the stoichiometric model by adding kinetic information of growth-limiting substrate importers in the form of an irreversible Michaelis-Menten equation ( $v_{upt} = V_{max} \frac{[S]}{K_m + [S]}$ ), where  $v_{upt}$  represents the uptake reaction,  $V_{max}$  the maximum rate of the uptake reaction,  $[S]$  the substrate concentration and  $K_m$  the substrate affinity. At each time step in dFBA the biomass production rate for each organism is independently optimised based on the specific substrate uptake rate. Implementing such dynamic uptake reaction enables the model to respond to changes in external concentrations.

For the simulations we use a genome-scale metabolic model for the metabolism of *C. acetobutylicum* and for *W. succinogenes* a coarse-grained model, which lumps metabolic segments into single reactions. We used a coarse-grained model as we expected that we could model our results without the need for full genome-scale reconstruction. We did do the reconstruction to verify that this was indeed the case (see supplemental material). Having a coarse-grained model facilitates computation and interpretation, especially if these methods are applied to larger and more complex microbial ecosystems.

Conversely, the detailed model of *C. acetobutylicum* has the advantage that it captures changes in its metabolism, as we observed that final acetate and butyrate concentrations, produced by *C. acetobutylicum* changes when the growth medium was varied. Another advantage is that it describes the metabolic flexibility associated with  $\text{H}_2$  production by *C. acetobutylicum* and leads to oxidization of ferredoxin. Ferredoxin is a conserved moiety whose total

concentration does not change (only its redox state), and when it is oxidized by another reaction, it will result in decreased H<sub>2</sub> production. Since *C. acetobutylicum* contains several reactions that can oxidize or reduce ferredoxin, the H<sub>2</sub> production flux is flexible, influencing the community interactions that we aim to quantify. For instance, NO<sub>2</sub><sup>-</sup> uptake decreases the amount of H<sub>2</sub> production, because both reactions require ferredoxin, which results in potential interesting dynamics between the two species, because *W. succinogenes* provides NO<sub>2</sub><sup>-</sup>, but requires H<sub>2</sub> which is produced by *C. acetobutylicum*. Several genome-scale metabolic models of *C. acetobutylicum* are available [32, 33]. We decided to use the model created by Salimi and co-workers [13], because this model was already successfully used for dFBA simulations.

We constructed a coarse-grained model of the core metabolism of *W. succinogenes*, containing eight reactions (S1 Table) that was detailed enough to fit the exchange fluxes to experimental data; the data indicated that *C. acetobutylicum* shows most metabolic flexibility. The ATP yield of NO<sub>3</sub><sup>-</sup> reduction, when H<sub>2</sub> is oxidized, was taken from literature [34]. We fitted the elemental composition of *W. succinogenes* biomass. It can use acetate as a carbon source [35], but with an unknown biomass yield. Similarly the NH<sub>4</sub><sup>+</sup> and ATP requirements for the production of one unit of biomass are unclear. We estimated all these values by varying them and used those values that resulted in the best fit with the experimental data. An advantage of working with coarse-grained models is that the model complexity is greatly reduced and the degrees of freedom are limited, whereas in genome-scale metabolic models these can increase rapidly [36–38]. However, we also constructed a draft genome-scale metabolic model of *W. succinogenes* to compare the results from the simulations with this model with the coarse-grained model (S1 File).

The two metabolic models were coupled through exchange fluxes for H<sub>2</sub>, NO<sub>2</sub><sup>-</sup> and acetate. The co-culture model was manually fitted to the experimental data, using dFBA, to infer the metabolic exchange fluxes in the microbial community. Manually fitting was done by changing the kinetic parameters (S2 Table), biomass composition of *W. succinogenes* (S1 Table) and ratio of acetate/butyrate production and NH<sub>4</sub><sup>+</sup>/NO<sub>2</sub><sup>-</sup> consumption until the simulation agreed most with the experimental data. ame

## The metabolic models can simulate the experimental data

Once the simulations agree with the experimental data, the corresponding metabolic fluxes can be extracted from the simulations, including the exchange fluxes between the two species. This allows us to infer the metabolic interactions between species in a microbial community.

To fit the model with the experiments, we varied the parameters of the models (S2 Table) to find an optimal fit. These parameters influence the rate of consumption and production of the metabolites in the co-cultures and can be different between the various environmental conditions. For instance, the  $V_{max}$  of glucose uptake in *C. acetobutylicum* changes between the different conditions (S2 Table). Although the parameters can change between the conditions, we did not change the metabolic models itself. The structure of the metabolic models, therefore, remain identical between the different environmental conditions.

For *C. acetobutylicum*, we had to constrain the ratio of butyrate and acetate production fluxes and the ratio of the NH<sub>4</sub><sup>+</sup> and NO<sub>2</sub><sup>-</sup> consumption to fit the experimental data (S2 Table). Removing those ratios resulted in incorrect simulation of the metabolic profiles, which is the result of apparent suboptimal behaviour of *C. acetobutylicum*. One reason for this could be that H<sub>2</sub> inhibits certain reactions and results in suboptimal behavior. Several studies showed that H<sub>2</sub> affects the metabolism of *Clostridia* species [30, 39]. An other reason could be that there is a yield/rate trade-off and a high growth rate would result in a suboptimal biomass yield as observed for other organisms. Flux balance analysis will always find the flux

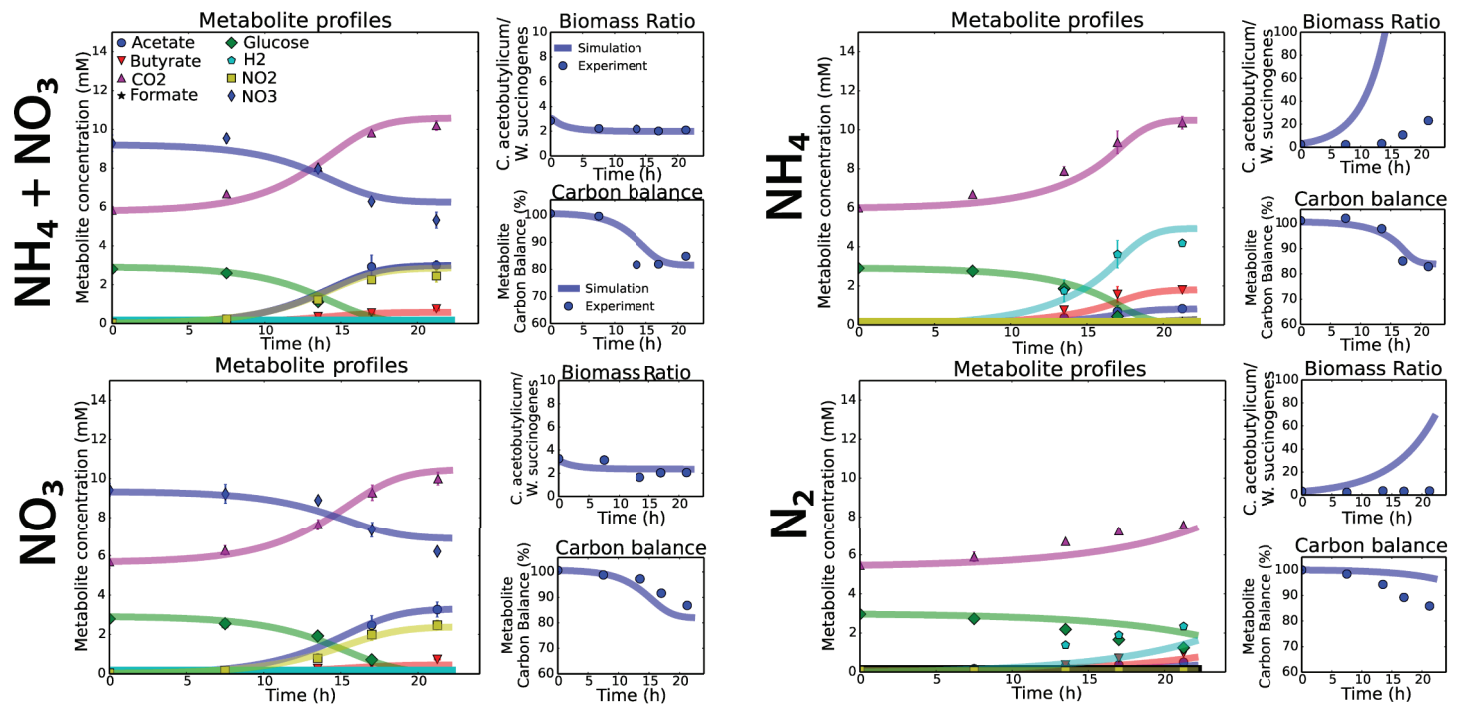


**Fig 3. The dFBA simulations agree mostly with the experimental data for the four different cultivation conditions and were used to infer the metabolic fluxes.** The metabolite profile plots contain error bars, but the other subplots not. The biomass ratios are based on the gene-copy data and the carbon balance consisted of the measured metabolites that contained carbon. The remaining missing carbon is assumed to be incorporated into biomass.

doi:10.1371/journal.pone.0173183.g003

distribution that maximizes this yield, not the rate. We also had to fit  $V_{max}$  and  $K_m$  of glucose uptake by *C. acetobutylicum* and the  $V_{max}$  and  $K_m$  of  $H_2$  uptake by *W. succinogenes* (S2 Table).

The simulation with the metabolic models are consistent with the experimental data, except that *W. succinogenes* grew in the absence of  $NO_3^-$ , which was not predicted with the model (Fig 3). This is most likely caused by carry-over of  $NO_3^-$  from the pre-culture and by cell lysis. However, these phenomena were not taken into account in the simulations of the metabolic model and therefore, no growth of *W. succinogenes* was predicted with the metabolic models (Fig 4B and 4D). Simulations where the genome-scale metabolic model of *W. succinogenes* was used were similar relative to the simulations with the coarse-grained model of *W. succinogenes* (S1 File).

### Influence of environmental conditions on the metabolic exchange fluxes between *C. acetobutylicum* and *W. succinogenes*

Simulations with the fitted model indicates that the growth rates of *C. acetobutylicum* and *W. succinogenes* are dynamic during the experiment (Fig 4). The biomass yields on substrate, however, remain constant during the whole experiment (S2 Fig). The dynamic behaviour of the community resulted therefore solely from the interplay between the dynamic concentrations of the environmental nutrients and products and the biomass abundances.

*W. succinogenes* grew faster than *C. acetobutylicum* in the first 10 hours in the presence of  $NH_4^+$  and  $NO_3^-$ . This is possible, because *C. acetobutylicum* is more abundant than *W. succinogenes* and can provide excess  $H_2$  despite the slower growth of *C. acetobutylicum*. After 10

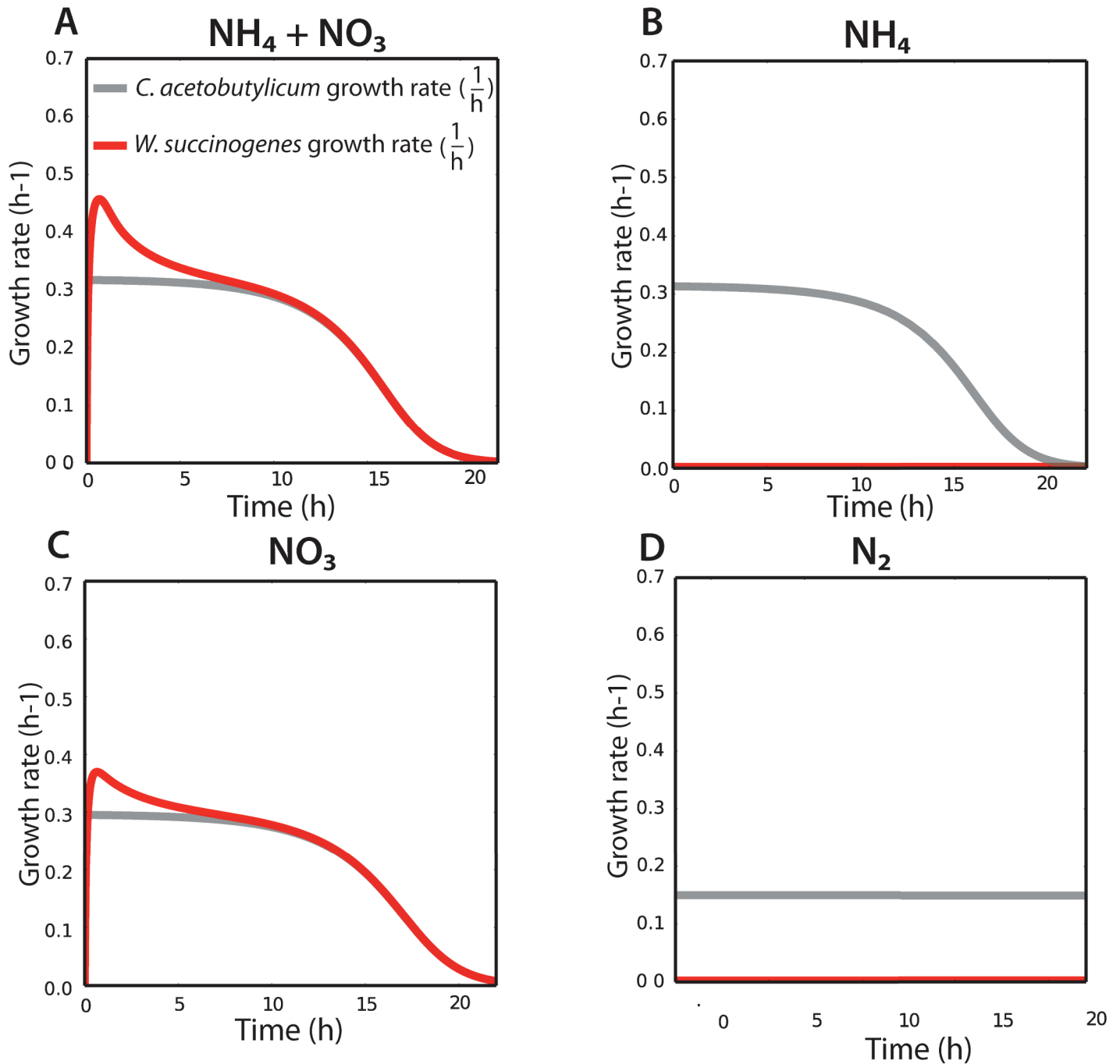


**Fig 4. Growth of *W. succinogenes* was limited by the growth-rate of *C. acetobutylicum*, based on the inferred growth-rates.** Balanced growth was observed after 10 hours of cultivation in the  $\text{NH}_4^+ + \text{NO}_3^-$  (A) and  $\text{NO}_3^-$  conditions (C). No growth of *W. succinogenes* was simulated in the  $\text{NH}_4^+$  (B) and  $\text{N}_2$  conditions (D).

doi:10.1371/journal.pone.0173183.g004

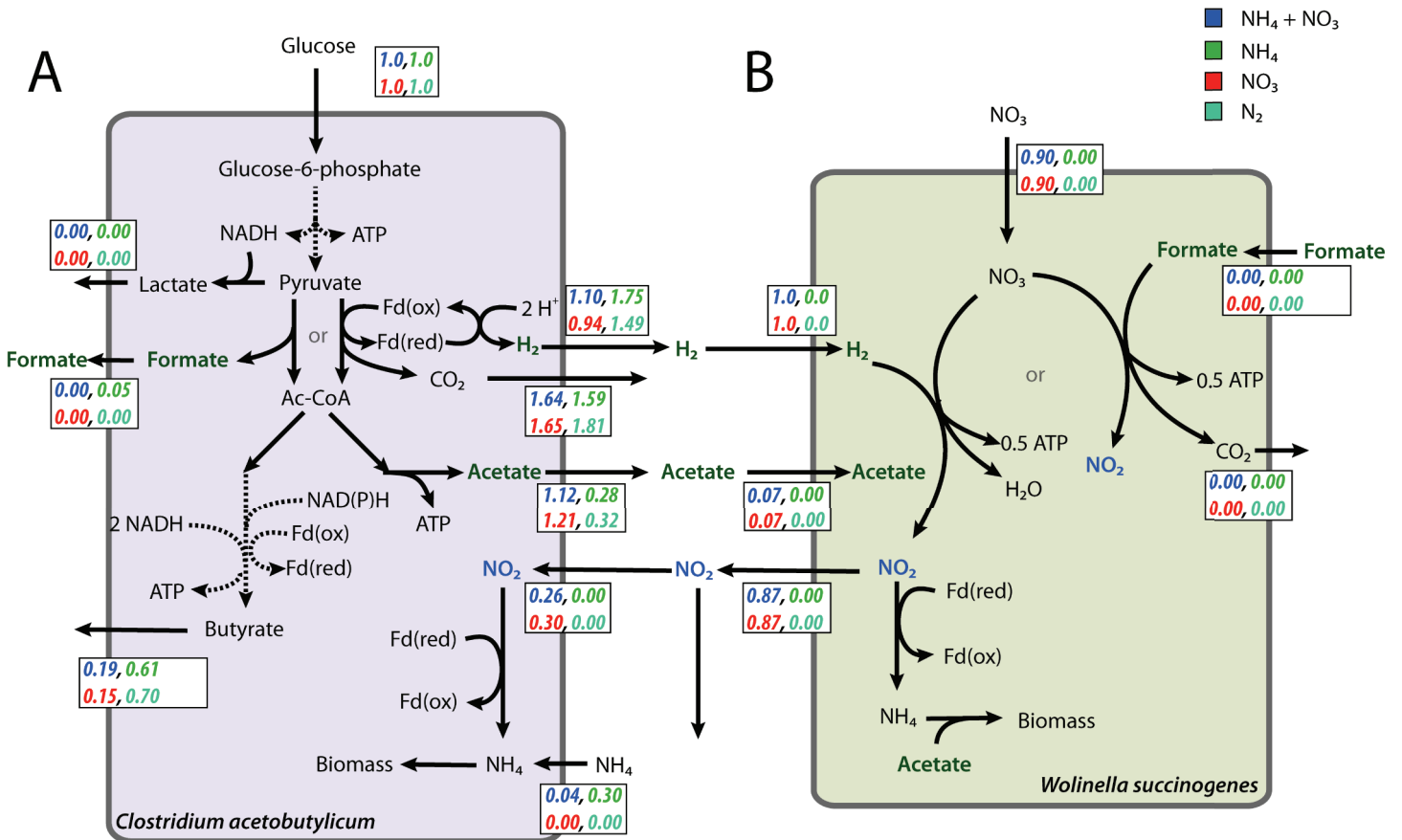


**Fig 5. Nitrogen-source also had an impact on the  $\text{H}_2$  and the  $\text{NO}_2^-$  exchange rates.** In **A** the calculated flux-values for *C. acetobutylicum* are normalized for the glucose uptake. **B** shows the calculated flux-values for *W. succinogenes* and are normalized for the  $\text{H}_2$  uptake. Note that  $\text{H}_2$  production by *C. acetobutylicum* is not equal to the specific  $\text{H}_2$  uptake rate of *W. succinogenes* as the biomass abundances should be taken into account, which were not equal during the experiment.

doi:10.1371/journal.pone.0173183.g005

hours, both species grew at the same specific rate. This is reflected in the experimental data of the biomass ratios of *C. acetobutylicum*/*W. succinogenes*, which decreased in the first hours of the experiment suggesting that *W. succinogenes* grows faster than *C. acetobutylicum*. This indicates that *C. acetobutylicum* determined the growth-rate of the community, because  $\text{H}_2$  consumption of *W. succinogenes* was limited by the  $\text{H}_2$  production of *C. acetobutylicum* after ten hours of cultivation.

Different nitrogen sources lead to changed metabolic interactions between *C. acetobutylicum* and *W. succinogenes* (Fig 5). The  $\text{H}_2$  production rate of *C. acetobutylicum*, during cultivation in the presence of  $\text{NO}_3^-$ , differed between the conditions: 1.10 and 0.94 mol/mol  $\text{H}_2$  per consumed glucose, for the ' $\text{NH}_4^+ + \text{NO}_3^-$ ' and ' $\text{NO}_3^-$ ' condition, respectively.  $\text{H}_2$  production was reduced by 17% in the ' $\text{NO}_3^-$ ' condition relative to the ' $\text{NH}_4^+ + \text{NO}_3^-$ ' condition.  $\text{H}_2$  is associated with oxidization of ferredoxin and this ferredoxin is also oxidized when  $\text{NO}_2^-$  is reduced to  $\text{NH}_4^+$ . Since ferredoxin is a conserved moiety, an increase in the  $\text{NO}_2^-$  reduction flux causes a lower  $\text{H}_2$  production flux, which occurred in the ' $\text{NO}_3^-$ ' condition. Therefore, there is an interesting dynamic between *C. acetobutylicum* and *W. succinogenes* when  $\text{NO}_3^-$  is in the medium, because *C. acetobutylicum* can use its ferredoxin for the production of  $\text{H}_2$ , but

also for the consumption of  $\text{NO}_2^-$ , which is produced by *W. succinogenes*. We show that the nitrogen source can have implications for interspecies hydrogen transfer in a community. An oxidized nitrogen source, in this case  $\text{NO}_2^-$ , would decrease  $\text{H}_2$  transfer and therefore  $\text{NH}_4^+$  is the preferred substrate for maximization of interspecies hydrogen transfer. Contrary to our expectations, a combination of  $\text{NH}_4^+$  and  $\text{NO}_2^-$  is predicted to be utilized by *C. acetobutylicum* in the  $\text{NH}_4^+ + \text{NO}_3^-$  condition. One explanation for *C. acetobutylicum*'s utilization of  $\text{NO}_2^-$  is to detoxify the medium. High  $\text{NO}_2^-$  concentrations inhibit growth and utilizing  $\text{NO}_2^-$  as a nitrogen source could be a detoxification strategy [40].

In contrast to the inferred fluxes of *C. acetobutylicum*, the inferred fluxes of *W. succinogenes* were equal between the ' $\text{NH}_4^+ + \text{NO}_3^-$ ' and ' $\text{NO}_3^-$ ' conditions (Fig 5B), suggesting that *W. succinogenes* was insensitive to the change in environmental conditions. This is primarily due to the limited flexibility of the model of *W. succinogenes*; however, the model fits with the experimental data, which suggests that the inferred fluxes are realistic. The simulations with the draft genome-scale metabolic model of *W. succinogenes* showed similar results relative to the coarse-grained model, except that the amount of consumed  $\text{NO}_3^-$  and produced  $\text{NO}_2^-$  per  $\text{H}_2$  was different (S3 Fig). This is primarily caused by the nitrogen and energy requirements for the production of biomass and is different for both models. We expect that a more accurate biomass function for the genome-scale metabolic model of *W. succinogenes* would improve the results.

### Intracellular fluxes of *C. acetobutylicum* can be inferred from community-level experimental data

In addition to calculation of the uptake and production fluxes, the genome-scale metabolic model of *C. acetobutylicum* informs us about intracellular flux values across the different conditions. This gives additional information about the active metabolic pathways. Due to the large number of reactions in the genome-scale metabolic model, the predicted values of the intracellular fluxes in the metabolic network are likely underdetermined, because we have too few experimental data to constrain those fits sufficiently.

We therefore performed a Flux Variability Analysis (FVA) [26], to check whether alternative intracellular flux values of the *C. acetobutylicum* metabolic network could fit the experimental data equally well. This analysis indicates a small flexibility, only 41 reactions of the 744 reactions had variable values (5.5%) ([https://sourceforge.net/projects/cbmpy/files/publications/data/2017\\_Hanemaaijer/](https://sourceforge.net/projects/cbmpy/files/publications/data/2017_Hanemaaijer/)). Those 41 reactions are involved in either malate cycling, proline and nucleotide biosynthesis, and carry very small fluxes relative to the fluxes in *C. acetobutylicum*'s core-metabolism. Two reactions that did carry a high flux are involved in ferredoxin cycling, but had no impact on the  $\text{H}_2$  production flux. There was also no variability identified in other uptake or production fluxes. These results suggest that in our system, the calculated flux distribution within *C. acetobutylicum* can be robustly predicted from community-level experimental data alone.

### Modelling predicts that co-culture behaviour can be enhanced

Besides providing a method for inferring experimental fluxes from experimental data, the metabolic model can also be used to predict the optimal behaviour of the community when not constrained with experimental data. Optimisation informs us about optimal metabolic coupling between the microorganisms when growth of both species are optimised.

Here, we consider the co-culture as optimal when the growth rates of both organisms are maximal. In dFBA this means that we optimise the flux towards biomass of both organisms on the supplied nutrients to the community. We determined the metabolic fluxes (internal and

exchange), growth rate and biomass abundances corresponding to the optimal state in the 'NH<sub>4</sub><sup>+</sup> + NO<sub>3</sub><sup>-</sup>' and 'NO<sub>3</sub><sup>-</sup>' condition when we released the constraints on the butyrate/acetate production ratio and the NH<sub>4</sub><sup>+</sup>/NO<sub>2</sub><sup>-</sup> consumption ratio of *C. acetobutylicum* (Fig 6).

The model predicted that an optimal *C. acetobutylicum* would have a changed metabolism relative to the experimental data. For instance, acetate rather than butyrate should be produced when *C. acetobutylicum* grows optimally. This behaviour was seen both in the 'NH<sub>4</sub><sup>+</sup> + NO<sub>3</sub><sup>-</sup>' and the 'NO<sub>3</sub><sup>-</sup>' condition. The explanation is that more ATP can be generated from acetate production than from butyrate production. An optimal *C. acetobutylicum* would not consume NO<sub>2</sub><sup>-</sup> when growing at the 'NH<sub>4</sub><sup>+</sup> + NO<sub>3</sub><sup>-</sup>' condition, because NO<sub>2</sub><sup>-</sup> reduction by nitrite reductase decreases growth of *C. acetobutylicum* according to the metabolic model. As explained, the amount of H<sub>2</sub> produced is inversely related with the amount of NO<sub>2</sub><sup>-</sup> taken up. As a consequence, 159% more H<sub>2</sub> was produced in the optimal scenario relative to the experiments in the 'NH<sub>4</sub><sup>+</sup> + NO<sub>3</sub><sup>-</sup>' condition. A smaller increase in H<sub>2</sub> production (+23%) was shown in the 'NO<sub>3</sub><sup>-</sup>' condition, suggesting that the interactions between the two species were not optimal in the experiments at those two conditions. However, the experimental growth-rate of *C. acetobutylicum* was close to its maximal, computed value. For the 'NH<sub>4</sub><sup>+</sup> + NO<sub>3</sub><sup>-</sup>' the experimental growth rate was 87% of the optimal value, whereas for the 'NO<sub>3</sub><sup>-</sup>' this was 94%. These results suggest that the experimental behaviour of the community with imposed bidirectional interactions is closer to the optimal metabolic behaviour than a community with unidirectional interactions.

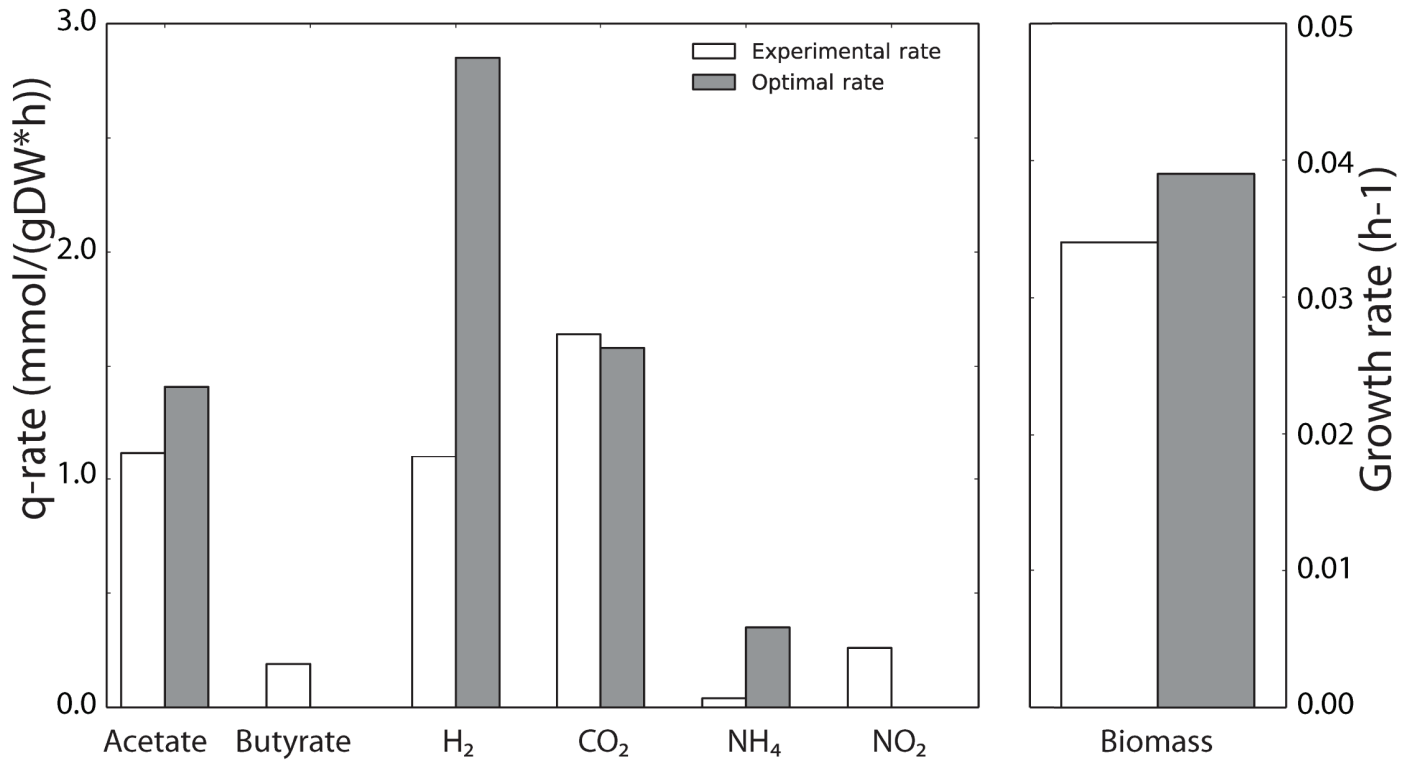
## Discussion

In this study we showed that the combination of a stoichiometric metabolic model with measured community-level concentrations and biomass abundances allows for the inference of metabolic interactions in a microbial community. This approach is complementary with current approaches that are based on correlation or co-occurrence networks, which predicts the community-interaction structure for large complex ecosystems [5, 41, 42]. These networks identify co-occurrence of species, suggesting that certain species in an ecosystem form a positive relationship with each other. However, the mechanisms behind the interactions remain unknown; here we infer them with metabolic models.

Stoichiometric models of metabolism make inference of metabolic exchange fluxes possible because they relate the uptake and production of environmental metabolites, to intracellular metabolic fluxes, organism abundance and growth rate. Such models are therefore integrating heterogeneous data types from which we make inferences about community behaviour. In addition to experimental data of species abundances and metabolite concentrations, molecular data can be used in the construction of stoichiometric metabolic models [43–45]. It is the integrative capability of stoichiometric models that makes them so useful for addressing current challenges in microbial ecology.

Metabolic models have been used to predict the behaviour of industrially relevant co-cultures and the type of interactions required to predict this behaviour [13, 14]. We show that this approach also works for ecologically relevant communities, where interspecies hydrogen transfer is the dominating interaction. Additionally, not only the type of interactions is identified, but we also infer the size of the interactions from the experimental data. With this method we show that the nitrogen source plays an important role in the rate of H<sub>2</sub> exchange in our co-culture. Recently, Embree *et al.* [46] also inferred metabolic interactions of a microbial community, but optimized each species individually as a steady-state simulation and did not combine all metabolic models into one community. We, on the other hand, simulated the dynamics of the co-culture, because we fitted data from a dynamic system where species could

# NH<sub>4</sub> + NO<sub>3</sub>



# NO<sub>3</sub>

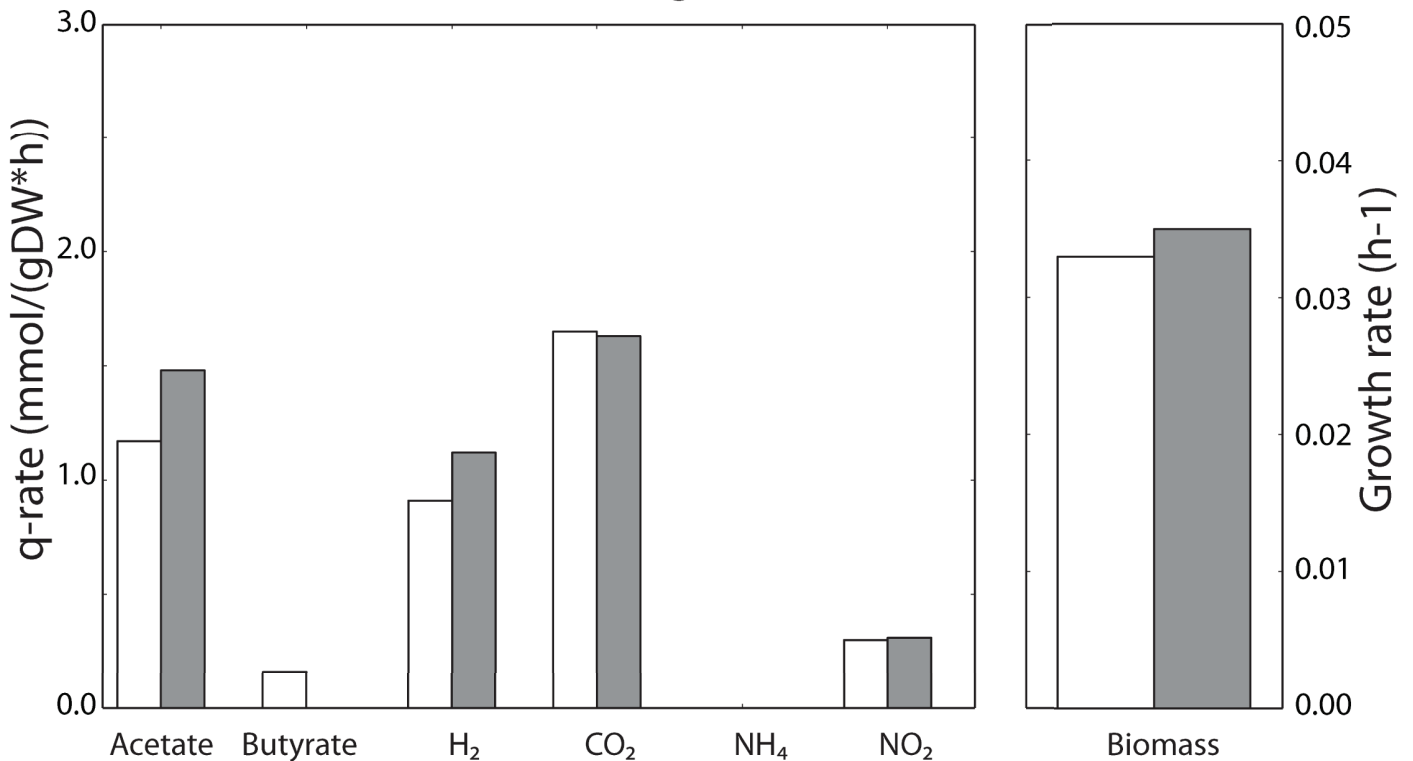


**Fig 6. The 'NO<sub>3</sub><sup>-</sup>' condition behaved more optimal than the 'NH<sub>4</sub><sup>+</sup> + NO<sub>3</sub><sup>-</sup>' condition.** The calculated experimental specific uptake and consumption rates (mmol/(gDW·h)) for *C. acetobutylicum* (white bars) and the *in-silico* optimal rates (gray bars) were compared. All specific uptake and production fluxes were normalized to the specific glucose uptake rate.

doi:10.1371/journal.pone.0173183.g006

change their metabolic behaviour during the experiment, which is closer to natural environments.

We have shown that our approach works for a co-culture and a next step would be the inference of metabolic interactions in a complex ecosystem. A complex community will have more interactions between the members of the community. In addition to beneficial relationships, competition can also play an important role in microbial communities [1]. The advantage of our dFBA based approach is that these type of interactions can also be inferred. Moreover, our results indicate that it is not even necessary to use full-blown genome-scale stoichiometric models for all members of a complex community as a coarse-grained model of *W. succinogenes* sufficed for the inference of metabolic interactions, as we recently suggested [7]. More detail can always be added later to refine predictions or resolve discrepancies, depending on the research question and data at hand.

Even though metabolic interactions can be inferred from experimental data, not all data and systems are equally amenable to a modeling approach. Firstly, a community with growing micro-organisms is advantageous. Growing cells have an active metabolism and increase their biomass in time, while interacting with other species. While non-growing species may also have an active metabolism, they do not increase in biomass, causing them to have lower fluxes, which makes it difficult to assign flux-values to such organisms. Secondly, controlled environments allow for more targeted perturbations of the community. Manipulation of the environment results in different dominating processes in the ecosystem [47]. In addition, a basic understanding of the core metabolism of the studied organisms is required. In our system, we had already an idea what type of interactions would take place, but this will not always be possible with complex ecosystems with poorly studied microorganisms. In such cases, metabolic reconstruction based on complete genomes is the best option to get a hint at the basic metabolic capacities. Lastly, a medium that is well-defined and minimal, is advantageous. Metabolites, which are turned over, are more easily identified in such media. A medium which, for instance, contains yeast extract provides all types of vitamins, amino acids and carbon compounds to the community members, and could mask or compromise the metabolic interactions in the ecosystem. With improved analytics, such challenges may be overcome, and we believe in view of the complexity of microbial communities, metabolic models are a promising and arguable the only- tool for the inference of the metabolic interactions of co-cultures.

To conclude, in our eyes metabolic models are an indispensable tool for the inference of the metabolic interactions, as illustrated with our co-culture study. We have shown that the nitrogen-source quantitatively influences the interspecies hydrogen transfer, which was not feasible with experimental data alone. Moreover, the metabolic models can be used for more purposes than inference of metabolic interactions. They can also be used to infer the intracellular fluxes of species, which informs us about the metabolic adaptations of microorganisms, during different conditions. The models can also be used to investigate whether species in a community grow optimally or whether they are limited by external factors. This is particularly interesting for communities used for industrial processes, such as the anaerobic digestion process, where high biogas yields are desired. Finally, metabolic models could indicate strategies to steer the community in a desired direction, guiding community engineering approaches. Thus

metabolic models have great potential –are simply required– to study complex, microbial ecosystems.

## Supporting information

### S1 Material and Methods.

(PDF)

**S1 Table. A coarse-grained metabolic model of *W. succinogenes* was detailed enough to fit the experimental data.** All metabolites, except for  $H^+$  and  $H_2O$ , are element-balanced in the metabolic model.

(PDF)

### S2 Table. Parameters used for simulation of the co-culture.

(PDF)

**S1 Fig. The dFBA simulations, with the draft genome-scale metabolic model of *W. succinogenes*, also agree mostly with the experimental data for the four different cultivation conditions.** The metabolite profile plots contain error bars, but the other subplots not. The biomass ratios are based on the gene-copy data and the carbon balance consisted of the measured metabolites that contained carbon. The remaining missing carbon is assumed to be incorporated into biomass.

(EPS)

**S2 Fig. Product and substrate yields did not change during different growth rates.** The extracted specific uptake and production rates (mmol/(gDW·h)) are plotted against the simulated growth rate  $\mu$  (h<sup>-1</sup>). All lines are linear what suggests that the specific uptake and production rates of both species are scaled with the growth. The  $N_2$  condition is not plotted, because the simulated growth rate was constant over the whole simulation.

(EPS)

**S3 Fig. Inference of the metabolic interactions using a draft genome-scale metabolic model of *W. succinogenes* showed only differences in the  $NO_2^-$  production and  $NO_3^-$  consumption per utilized  $H_2$ .** In **A** the calculated flux-values for *C. acetobutylicum* are normalized for the glucose uptake. **B** shows the calculated flux-values for *W. succinogenes* and are normalized for the  $H_2$  uptake. Note that  $H_2$  production by *C. acetobutylicum* is not equal to the specific  $H_2$  uptake rate of *W. succinogenes* as the biomass abundances should be taken into account, which were not equal during the experiment.

(EPS)

**S1 File. Draft genome-scale metabolic model of *W. succinogenes*.** The reactions and the corresponding reversibility and bounds are listed in ‘reactions’. The metabolites-id and the corresponding names are listed in ‘metabolites’. All reactions and their corresponding substrates and products are listed in ‘network\_react’, where in ‘network\_metab’ all reactions per metabolite is listed. All metabolites and their corresponding MIRIAM information is listed in ‘miriam.’

(XLS)

## Acknowledgments

This work is financially supported by ZonMW and the Netherlands Genomics Initiative via a Zenith Horizon grant 40-41009-98-10038. BGO is supported by a BE-Basic Foundation grant F08.005.001.

## Author Contributions

**Conceptualization:** MH WR FB BT.

**Formal analysis:** MH BO.

**Funding acquisition:** BT.

**Investigation:** MH.

**Methodology:** MH BO.

**Project administration:** WR BT.

**Software:** BO.

**Supervision:** WR BT.

**Validation:** MH.

**Visualization:** MH.

**Writing – original draft:** MH FB.

**Writing – review & editing:** MH BO FB BT.

## References

1. Coyte KZ, Schluter J, Foster KR. The ecology of the microbiome: Networks, competition, and stability. *Science*. 2015; 350(6261):663–666. doi: [10.1126/science.aad2602](https://doi.org/10.1126/science.aad2602) PMID: [26542567](https://pubmed.ncbi.nlm.nih.gov/26542567/)
2. De Vuyst L, Neysens P. The sourdough microflora: biodiversity and metabolic interactions. *Trends in Food Science & Technology*. 2005; 16(1):43–56. doi: [10.1016/j.tifs.2004.02.012](https://doi.org/10.1016/j.tifs.2004.02.012)
3. Møller S, Sternberg C, Andersen JB, Christensen BB, Ramos JL, Givskov M, et al. In situ gene expression in mixed-culture biofilms: evidence of metabolic interactions between community members. *Applied and environmental microbiology*. 1998; 64(2):721–732. PMID: [9464414](https://pubmed.ncbi.nlm.nih.gov/9464414/)
4. Stams AJ. Metabolic interactions between anaerobic bacteria in methanogenic environments. *Antonie van Leeuwenhoek*. 1994; 66(1-3):271–294. doi: [10.1007/BF00871644](https://doi.org/10.1007/BF00871644) PMID: [7747937](https://pubmed.ncbi.nlm.nih.gov/7747937/)
5. Faust K, Sathirapongsasuti JF, Izard J, Segata N, Gevers D, Raes J, et al. Microbial co-occurrence relationships in the human microbiome. *PLoS Comput Biol*. 2012; 8(7):e1002606–e1002606. doi: [10.1371/journal.pcbi.1002606](https://doi.org/10.1371/journal.pcbi.1002606) PMID: [22807668](https://pubmed.ncbi.nlm.nih.gov/22807668/)
6. Barberán A, Bates ST, Casamayor EO, Fierer N. Using network analysis to explore co-occurrence patterns in soil microbial communities. *The ISME journal*. 2012; 6(2):343–351. doi: [10.1038/ismej.2011.119](https://doi.org/10.1038/ismej.2011.119) PMID: [21900968](https://pubmed.ncbi.nlm.nih.gov/21900968/)
7. Hanemaaijer M, Røling WF, Olivier BG, Khandelwal RA, Teusink B, Bruggeman FJ. Systems modeling approaches for microbial community studies: from metagenomics to inference of the community structure. *Frontiers in microbiology*. 2015; 6. doi: [10.3389/fmicb.2015.00213](https://doi.org/10.3389/fmicb.2015.00213) PMID: [25852671](https://pubmed.ncbi.nlm.nih.gov/25852671/)
8. Zengler K, Palsson BO. A road map for the development of community systems (CoSy) biology. *Nature Reviews Microbiology*. 2012; 10(5):366–372. PMID: [22450377](https://pubmed.ncbi.nlm.nih.gov/22450377/)
9. Røling WF, van Bodegom PM. Toward quantitative understanding on microbial community structure and functioning: a modeling-centered approach using degradation of marine oil spills as example. *Frontiers in microbiology*. 2014; 5. doi: [10.3389/fmicb.2014.00125](https://doi.org/10.3389/fmicb.2014.00125) PMID: [24723922](https://pubmed.ncbi.nlm.nih.gov/24723922/)
10. Klitgord N, Segre D. Ecosystems biology of microbial metabolism. *Current opinion in biotechnology*. 2011; 22(4):541–546. doi: [10.1016/j.copbio.2011.04.018](https://doi.org/10.1016/j.copbio.2011.04.018) PMID: [21592777](https://pubmed.ncbi.nlm.nih.gov/21592777/)
11. Levy R, Borenstein E. Metabolic modeling of species interaction in the human microbiome elucidates community-level assembly rules. *Proceedings of the National Academy of Sciences*. 2013; 110(31):12804–12809. doi: [10.1073/pnas.1300926110](https://doi.org/10.1073/pnas.1300926110) PMID: [23858463](https://pubmed.ncbi.nlm.nih.gov/23858463/)
12. Stolyar S, Van Dien S, Hillesland KL, Pinel N, Lie TJ, Leigh JA, et al. Metabolic modeling of a mutualistic microbial community. *Molecular systems biology*. 2007; 3(1). doi: [10.1038/msb4100131](https://doi.org/10.1038/msb4100131) PMID: [17353934](https://pubmed.ncbi.nlm.nih.gov/17353934/)

13. Salimi F, Zhuang K, Mahadevan R. Genome-scale metabolic modeling of a clostridial co-culture for consolidated bioprocessing. *Biotechnology journal*. 2010; 5(7):726–738. doi: [10.1002/biot.201000159](https://doi.org/10.1002/biot.201000159) PMID: [20665645](https://pubmed.ncbi.nlm.nih.gov/20665645/)
14. Hanly TJ, Henson MA. Dynamic flux balance modeling of microbial co-cultures for efficient batch fermentation of glucose and xylose mixtures. *Biotechnology and bioengineering*. 2011; 108(2):376–385. doi: [10.1002/bit.22954](https://doi.org/10.1002/bit.22954) PMID: [20882517](https://pubmed.ncbi.nlm.nih.gov/20882517/)
15. Heinken A, Sahoo S, Fleming RM, Thiele I. Systems-level characterization of a host-microbe metabolic symbiosis in the mammalian gut. *Gut microbes*. 2013; 4(1):3–15. doi: [10.4161/gmic.22370](https://doi.org/10.4161/gmic.22370) PMID: [23022739](https://pubmed.ncbi.nlm.nih.gov/23022739/)
16. Klitgord N, Segre D. Environments that induce synthetic microbial ecosystems. *PLoS Comput Biol*. 2010; 6(11):e1001002. doi: [10.1371/journal.pcbi.1001002](https://doi.org/10.1371/journal.pcbi.1001002) PMID: [21124952](https://pubmed.ncbi.nlm.nih.gov/21124952/)
17. Khandelwal RA, Olivier BG, Röling WF, Teusink B, Bruggeman FJ. Community Flux Balance Analysis for Microbial Consortia at Balanced Growth. *PloS one*. 2013; 8(5):e64567. doi: [10.1371/journal.pone.0064567](https://doi.org/10.1371/journal.pone.0064567) PMID: [23741341](https://pubmed.ncbi.nlm.nih.gov/23741341/)
18. Wittebolle L, Marzorati M, Clement L, Balloi A, Daffonchio D, Heylen K, et al. Initial community evenness favours functionality under selective stress. *Nature*. 2009; 458(7238):623–626. doi: [10.1038/nature07840](https://doi.org/10.1038/nature07840) PMID: [19270679](https://pubmed.ncbi.nlm.nih.gov/19270679/)
19. Pawelczyk S, Abraham WR, Harms H, Müller S. Community-based degradation of 4-chlorosalicylate tracked on the single cell level. *Journal of microbiological methods*. 2008; 75(1):117–126. doi: [10.1016/j.mimet.2008.05.018](https://doi.org/10.1016/j.mimet.2008.05.018) PMID: [18593643](https://pubmed.ncbi.nlm.nih.gov/18593643/)
20. Patle S, Lal B. Ethanol production from hydrolysed agricultural wastes using mixed culture of *Zymomonas mobilis* and *Candida tropicalis*. *Biotechnology letters*. 2007; 29(12):1839–1843. doi: [10.1007/s10529-007-9493-4](https://doi.org/10.1007/s10529-007-9493-4) PMID: [17657407](https://pubmed.ncbi.nlm.nih.gov/17657407/)
21. Yang J, Kim J, Skogley E, Schaff B. A simple spectrophotometric determination of nitrate in water, resin, and soil extracts. *Soil Science Society of America Journal*. 1998; 62(4):1108–1115. doi: [10.2136/sssaj1998.03615995006200040036x](https://doi.org/10.2136/sssaj1998.03615995006200040036x)
22. Lee SM, Cho MO, Um Y, Sang BI. Development of Real-Time PCR primer and probe sets for detecting degenerated and non-degenerated forms of the butanol-producing bacterium *Clostridium acetobutylicum* ATCC 824. *Applied biochemistry and biotechnology*. 2010; 161(1-8):75–83. doi: [10.1007/s12010-009-8788-4](https://doi.org/10.1007/s12010-009-8788-4) PMID: [19798472](https://pubmed.ncbi.nlm.nih.gov/19798472/)
23. Olivier BG, Bergmann FT. The Systems Biology Markup Language (SBML) Level 3 Package: Flux Balance Constraints. *Journal of integrative bioinformatics*. 2015; 12(2):269. doi: [10.2390/biecoll-jib-2015-269](https://doi.org/10.2390/biecoll-jib-2015-269) PMID: [26528567](https://pubmed.ncbi.nlm.nih.gov/26528567/)
24. Zhuang K, Izallalen M, Mouser P, Richter H, Risso C, Mahadevan R, et al. Genome-scale dynamic modeling of the competition between *Rhodospirillum rubrum* and *Geobacter* in anoxic subsurface environments. *The ISME journal*. 2010; 5(2):305–316. doi: [10.1038/ismej.2010.117](https://doi.org/10.1038/ismej.2010.117) PMID: [20668487](https://pubmed.ncbi.nlm.nih.gov/20668487/)
25. Jones E, Oliphant T, Peterson P. {SciPy}: Open source scientific tools for {Python}. 2014;.
26. Mahadevan R, Schilling C. The effects of alternate optimal solutions in constraint-based genome-scale metabolic models. *Metabolic engineering*. 2003; 5(4):264–276. doi: [10.1016/j.ymben.2003.09.002](https://doi.org/10.1016/j.ymben.2003.09.002) PMID: [14642354](https://pubmed.ncbi.nlm.nih.gov/14642354/)
27. Wilson P, Peterson W, Fred E. The relationship between the nitrogen and carbon metabolism of *Clostridium acetobutylicum*. *Journal of bacteriology*. 1930; 19(4):231. PMID: [16559425](https://pubmed.ncbi.nlm.nih.gov/16559425/)
28. Rosenblum ED, Wilson P. Fixation of isotopic nitrogen by *Clostridium*. *Journal of bacteriology*. 1949; 57(4):413. PMID: [18120606](https://pubmed.ncbi.nlm.nih.gov/18120606/)
29. Chen J, Toth J, Kasap M. Nitrogen-fixation genes and nitrogenase activity in *Clostridium acetobutylicum* and *Clostridium beijerinckii*. *Journal of Industrial Microbiology and Biotechnology*. 2001; 27(5):281–286. doi: [10.1038/sj.jim.7000083](https://doi.org/10.1038/sj.jim.7000083) PMID: [11781802](https://pubmed.ncbi.nlm.nih.gov/11781802/)
30. Chung KT. Inhibitory effects of H<sub>2</sub> on growth of *Clostridium cellobioparum*. *Applied and environmental microbiology*. 1976; 31(3):342–348. PMID: [779644](https://pubmed.ncbi.nlm.nih.gov/779644/)
31. Mahadevan R, Edwards JS, Doyle FJ III. Dynamic Flux Balance Analysis of Diauxic Growth in *Escherichia coli*. *Biophysical journal*. 2002; 83(3):1331–1340. doi: [10.1016/S0006-3495\(02\)73903-9](https://doi.org/10.1016/S0006-3495(02)73903-9) PMID: [12202358](https://pubmed.ncbi.nlm.nih.gov/12202358/)
32. Senger RS, Papoutsakis ET. Genome-scale model for *Clostridium acetobutylicum*: Part I. Metabolic network resolution and analysis. *Biotechnology and bioengineering*. 2008; 101(5):1036. doi: [10.1002/bit.22010](https://doi.org/10.1002/bit.22010) PMID: [18767192](https://pubmed.ncbi.nlm.nih.gov/18767192/)
33. Lee J, Yun H, Feist AM, Palsson BØ, Lee SY. Genome-scale reconstruction and in silico analysis of the *Clostridium acetobutylicum* ATCC 824 metabolic network. *Applied microbiology and biotechnology*. 2008; 80(5):849–862. doi: [10.1007/s00253-008-1654-4](https://doi.org/10.1007/s00253-008-1654-4) PMID: [18758767](https://pubmed.ncbi.nlm.nih.gov/18758767/)

34. Bokranz M, Katz J, Schröder I, Robertson AM, Kröger A. Energy metabolism and biosynthesis of *Vibrio succinogenes* growing with nitrate or nitrite as terminal electron acceptor. *Archives of Microbiology*. 1983; 135(1):36–41. doi: [10.1007/BF00419479](https://doi.org/10.1007/BF00419479)
35. Schumacher W, Kroneck PM, Pfennig N. Comparative systematic study on “*Spirillum*” 5175, *Campylobacter* and *Wolinella* species. *Archives of microbiology*. 1992; 158(4):287–293. doi: [10.1007/BF00245247](https://doi.org/10.1007/BF00245247)
36. Reed JL, Famili I, Thiele I, Palsson BO. Towards multidimensional genome annotation. *Nature Reviews Genetics*. 2006; 7(2):130–141. doi: [10.1038/nrg1769](https://doi.org/10.1038/nrg1769) PMID: [16418748](https://pubmed.ncbi.nlm.nih.gov/16418748/)
37. Teusink B, Wiersma A, Molenaar D, Francke C, de Vos WM, Siezen RJ, et al. Analysis of growth of *Lactobacillus plantarum* WCFS1 on a complex medium using a genome-scale metabolic model. *Journal of Biological Chemistry*. 2006; 281(52):40041–40048. doi: [10.1074/jbc.M606263200](https://doi.org/10.1074/jbc.M606263200) PMID: [17062565](https://pubmed.ncbi.nlm.nih.gov/17062565/)
38. Kelk SM, Olivier BG, Stougie L, Bruggeman FJ. Optimal flux spaces of genome-scale stoichiometric models are determined by a few subnetworks. *Scientific reports*. 2012; 2. doi: [10.1038/srep00580](https://doi.org/10.1038/srep00580) PMID: [22896812](https://pubmed.ncbi.nlm.nih.gov/22896812/)
39. Van Andel JG, Zoutberg GR, Crabbendam PM and Breure AM. Glucose fermentation by *Clostridium butyricum* grown under a self generated gas atmosphere in chemostat culture. *Applied microbiology and biotechnology*. 1985; 23(1):21–26. doi: [10.1007/BF02660113](https://doi.org/10.1007/BF02660113)
40. Ávila M, Gómez-Torres N, Hernández M, Garde S. Inhibitory activity of reuterin, nisin, lysozyme and nitrite against vegetative cells and spores of dairy-related *Clostridium* species. *International journal of food microbiology*. 2014; 172:70–75. doi: [10.1016/j.ijfoodmicro.2013.12.002](https://doi.org/10.1016/j.ijfoodmicro.2013.12.002) PMID: [24361835](https://pubmed.ncbi.nlm.nih.gov/24361835/)
41. Berry D, Widder S. Deciphering microbial interactions and detecting keystone species with co-occurrence networks. *Frontiers in microbiology*. 2014; 5. doi: [10.3389/fmicb.2014.00219](https://doi.org/10.3389/fmicb.2014.00219) PMID: [24904535](https://pubmed.ncbi.nlm.nih.gov/24904535/)
42. Zhou J, Deng Y, Luo F, He Z, Yang Y. Phylogenetic molecular ecological network of soil microbial communities in response to elevated CO<sub>2</sub>. *MBio*. 2011; 2(4):e00122–11. doi: [10.1128/mBio.00122-11](https://doi.org/10.1128/mBio.00122-11) PMID: [21791581](https://pubmed.ncbi.nlm.nih.gov/21791581/)
43. Åkesson M, Förster J, Nielsen J. Integration of gene expression data into genome-scale metabolic models. *Metabolic engineering*. 2004; 6(4):285–293. doi: [10.1016/j.ymben.2003.12.002](https://doi.org/10.1016/j.ymben.2003.12.002) PMID: [15491858](https://pubmed.ncbi.nlm.nih.gov/15491858/)
44. Maarleveld TR, Boele J, Bruggeman FJ, Teusink B. A data integration and visualization resource for the metabolic network of *Synechocystis* sp. PCC 6803. *Plant physiology*. 2014; p. pp–113.
45. Yizhak K, Benyamini T, Liebermeister W, Ruppin E, Shlomi T. Integrating quantitative proteomics and metabolomics with a genome-scale metabolic network model. *Bioinformatics*. 2010; 26(12):i255–i260. doi: [10.1093/bioinformatics/btq183](https://doi.org/10.1093/bioinformatics/btq183) PMID: [20529914](https://pubmed.ncbi.nlm.nih.gov/20529914/)
46. Embree M, Liu JK, Al-Bassam MM, Zengler K. Networks of energetic and metabolic interactions define dynamics in microbial communities. *Proceedings of the National Academy of Sciences*. 2015; 112(50):15450–15455. doi: [10.1073/pnas.1506034112](https://doi.org/10.1073/pnas.1506034112) PMID: [26621749](https://pubmed.ncbi.nlm.nih.gov/26621749/)
47. Kraft B, Tegetmeyer HE, Sharma R, Klotz MG, Ferdelman TG, Hettich RL, et al. The environmental controls that govern the end product of bacterial nitrate respiration. *Science*. 2014; 345(6197):676–679. doi: [10.1126/science.1254070](https://doi.org/10.1126/science.1254070) PMID: [25104387](https://pubmed.ncbi.nlm.nih.gov/25104387/)